Journal of
Computer & Electrical and Electronics Engineering Sciences
Original Article
DOI: 10.51271/JCEEES-0012

Hybrid charging station integration of solar power and IGBT technology for sustainable electric vehicle fast charging

Ferhat Kuzu[1], Atilla Ergüzen[2]

[1] Department of Defense Technologies, Institute of Science, Kırıkkale University, Turkiye
[2] Department of Computer Engineering, Faculty of Engineering, Kırıkkale University, Kırıkkale, Turkiye

Cite this article: Kuzu, F. & Ergüzen, A. (2024) Hybrid charging station integration of solar power and IGBT technology for sustainable electric vehicle fast charging. *J Comp Electr Electron Eng Sci*, 2(1), 5-16.

Corresponding Author: Ferhat Kuzu, ferhatkuzu08@gmail.com

Received: 17/01/2024 ◆ **Accepted**: 29/01/2024 ◆ **Published**: 27/04/2024

ABSTRACT

Aims: The aim of the study is to design a hybrid charging station that utilizes renewable energy sources, employs energy storage capabilities, incorporates insulated gate bipolar transistor (IGBT) technology, and provides a fast-charging solution. This design is intended to address the energy challenges arising from the widespread adoption of electric vehicles, offering a sustainable solution by harnessing renewable energy and storing it efficiently.

Methods: This study introduces a hybrid-charging station designed to address the charging needs of electric vehicles (EVs) and powered by renewable sources such as solar energy. The station utilizes IGBT technology in its rectifier section. Achieving an impressive 95% energy efficiency in 400 V direct current (DC) fast charging is experimentally validated. The charging process is initiated with energy derived from solar panels and nonstop transitions to battery or pulse width modulation (PWM) rectifier power as needed. The rectifier section employs the Sinusoidal PWM method for sampling a sinusoidal waveform, while pulse width modulation is used for the converter section by calculating the duty cycle.

Results: The hybrid charging station has demonstrated nonstop operation on both the grid and solar energy throughout the tests. The utilization of IGBT technology in the rectifier and converter sections contributes to achieving 400 V DC fast charging with a high energy efficiency rate of 95%. Parameters of the PWM rectifier and DC-DC converter have been simulated using MATLAB that is confirming the station's performance. Practical implementation has shown that values are close to the simulation.

Conclusion: The widespread use of fossil fuel-powered vehicles poses environmental and health risks due to carbon emissions. The increasing popularity of EVs addresses this concern, but challenges arise in charging infrastructure and grid suitability. This study proposes a hybrid charging station using PV modules and a storage unit with a DC-DC converter. Fast-charging capabilities and grid integration are included for non-solar periods. The system offers energy savings, has broad applications, and can operate independently, making it suitable for various scenarios. Future research can explore higher battery capacities, increased charging capabilities, and advanced technologies for optimal energy use.

Keywords: Hybrid charge station, DC and fast charge, renewable energy, photovoltaic (PV) system, PWM rectifier

INTRODUCTION

The innovation in transportation, initiated by the invention of internal combustion and electric motors due to the 19th-century industrial revolutions, is progressively intensifying energy demand. Vehicles commonly used in contemporary transportation with internal combustion engines rely on fossil fuel sources. One of the most significant disadvantages of internal combustion engine technology (Fossil fuels) is CO2 emission. According to a study conducted in the USA, 27% of all emissions originate from transportation (URL-1, 2021). The environmental damages caused by fossil fuels, their adverse effects on human health, and their limited reserves have heightened the societal demand for renewable energy sources as an alternative. Climate change and greenhouse gas emissions are experienced all over the world. The main reason behind them is the energy obtained from fossil fuels instead of renewable energy sources. Therefore, it is necessary to use renewable energy sources more actively (Çetintaş et al., 2017). Energy demand and consumption are increasing day by day, in parallel with population growth. Currently, a significant portion of the energy requirement is met from fossil sources. Fossil resources not only have limited capacity on Earth but also possess a specific reserve

This work is licensed under a Creative Commons Attribution 4.0 International License.

lifespan. Moreover, the utilization of fossil fuels is leading to a gradual acceleration of environmental and climatic issues. Individuals have become more conscious of the adverse impacts of fossil fuels on the environment and human health. Consequently, countries have begun to address a portion of their energy needs through renewable energy sources. Some renewable energy sources employed in these efforts include wind, solar, geothermal, hydro, and biomass energy (Gürbüz et al., 2021).

Compared to vehicles using fossil fuels, renewable energy sources are labeled clean energy that does not harm the environment. The increasing awareness of the environmental damage caused by carbon emissions from vehicles using fossil fuels, predominantly those with internal combustion engines, coupled with advancements in battery technologies, is steadily driving interest toward electric vehicles (EVs).

Consequently, EVs, exclusively equipped with electric motors, are becoming more prevalent each day. In line with the increasing use of EVs, energy requirements and charging infrastructure issues are gaining prominence. Research indicates that the energy demand for charging EVs imposes a significant burden on the grid, leading to adverse situations such as the increased use of power plants using fossil fuels to meet the growing demand for electrical energy. As a solution to this issue, gradual improvements should be made to address grid inadequacies and the utilization of renewable energy sources should be progressively increased.

The increase in EVs has triggered a growing demand for efficient and environmentally friendly charging solutions. In response to the need to limit greenhouse gas emissions and advance sustainable energy practices, there is an increasing interest in charging stations powered by renewable energy sources. This study presents an innovative hybrid charging station design that utilizes renewable energy for civilian and military EVs and features a fast-charging capability. The design is monitored in real-time with the assistance of a microcontroller, ensuring the system's shutdown in case of any issues. Additionally, batteries are employed as a storage unit to provide uninterrupted charging solutions. The detailed examination of the technical specifications of this charging station design, along with the utilization of simulation results, aims to realize the implementation of the design. When renewable energy-based hybrid charging stations are academically examined, charging methods, economical solutions, and decision-making mechanisms are categorized into various groups. Some of the studies that were conducted are listed below.

As per the U.S. Department of Energy (USDE), only 15% of the fuel used in internal combustion engine (ICE) cars is utilized for propelling the vehicle. Energy is lost in fossil fuel vehicles because it is dissipated as friction and heat in the moving system. While fossil fuel vehicles often require maintenance, EVs efficiently allocate over 75% of their energy towards propulsion. EVs typically offer an average range of 4 to 8 miles per kilowatt-hour (kWh) (Tie et al., 2013).

As depicted in Figure 1, electric cars are entirely powered by electricity. In contrast, as illustrated in Figure 2, hybrid cars feature two engines: one electric and one internal combustion. Hybrid vehicles utilize electricity for initial acceleration and switch to a fossil fuel source for other driving conditions. However, hybrid vehicles are not environmentally friendly due to their use of fossil fuels.

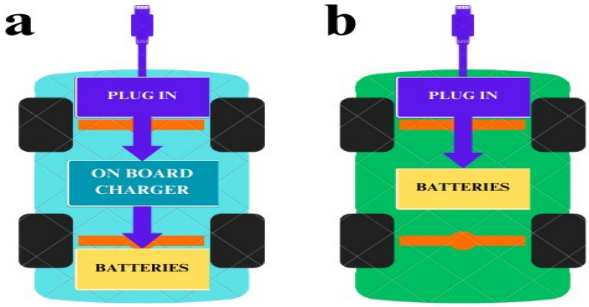

Figure 1. (a) AC charging; (b) DC fast charging

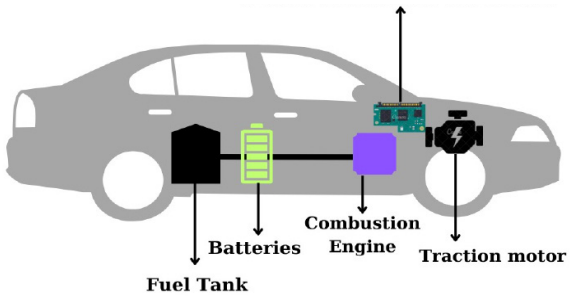

Figure 2. Hybrid car internal structure

Thanks to advances in battery technology, electric cars have now achieved the necessary range for practical use. As technology continues to evolve, these range distances are steadily increasing. In this way, EVs have started to replace hybrid vehicles in the market.

Electric cars do not have an internal combustion engine. For this reason, they do not create CO_2 gas emissions, which are harmful to the environment. It also does not cause noise pollution. It is more economical as it uses electrical energy as fuel. There are both household chargers and stationary charging stations for charging. The performance of EVs is higher than fossil fuel vehicles (Çetintaş et al., 2017).

The most significant disadvantage of electric vehicle (EV) charging due to solar panel (PV) charging is the variability in the desired PV production with intelligent charging. Intelligent charging can provide flexibility in EV chargers (Mouli et al., 2016). There are several methods to increase the driving range of an EV. The first is the battery capacity. The second goal is to reduce charging time to enhance usability. However, the structure limits the infrastructure dedicated to conductivity (where the AC-DC converter is included in the charging station) (Saber et al., 2017). EVs offer three critical capabilities for existing power plants: the ability to adjust charging power, rapid fluctuations in charging power and discharging capability. EV charging typically involves maintaining a constant power flow until the battery reaches total capacity (Mouli et al., 2017).

Standardizing existing charging stations, connection structures, and communication protocols enhances the quality and speed of charging for customers. This development makes the EV system more efficient,

contributing to widespread adoption worldwide. Various countries have established international standards to promote charging station development and broader use (Sutopo et al., 2018). Table 1 illustrates the EV standards of some countries.

Table 1. EV standards by country (Ng et al., 2011)

EV	Country
Society of Automotive Engineers (SAE)	USA
International Electrotechnical Commission (IEC)	Europe
Japanese Electrotechnical Committee (JEC)	Japan
China Electricity Council (CEC)	China

IEC 62196 is used as the standard in EV charging stations. Charging voltages are divided into alternative current (AC) and DC. It has been observed that the electric car charge voltages are examined at three different levels. It is the charging process with a standard socket without any safety precautions. There are three levels: level 1, 120 VAC charging method; level 2, 208-240 VAC charging method; and level 3, 208-850 VDC, respectively, fast charging method is applied. (Angelov et al., 2018). Charging is carried out with a single-phase/three-phase mains and grounding line. AC power supply line should be at most 32A, 250V AC (single phase), or 480VAC (Dericioglu et al., 2018). In the fast charge method, a charge rate of up to 70% in the vehicle battery can be reached with a 30-minute charge. In this method, the EV is connected to the AC mains supply by using a unique battery control system to control the devices in the battery system (IEC et al., 2010).

The design incorporates insulated gate bipolar transistor (IGBT) technology, providing advantages and disadvantages. The utilization of IGBT is evident in both the rectifier section and the DC-DC converter section, which features maximum power point tracking (MPPT) functionality. IGBT rectifier is a pulse width modulation (PWM) rectifier constructed using IGBTs (Gelman et al., 2014). A PWM rectifier offers the following advantages: adjustable DC voltage, energy recovery, power factor correction, and low harmonics (Hans et al., 1980). Rectifier switching activities initially employed silicon-controlled rectifiers (SCRs), followed by the adoption of gate turn-off thyristors (GTOs), and subsequently integrated with IGBTs. Significantly, advancements in IGBT technology have been made today, establishing it as a preferred device in converters covering the DC connection voltage range crucial for traction rectifiers (700 to 1500 VDC) (H. G. Eckel et al., 2005).

What distinguishes this study from other works is its capability to provide charging solutions for both military and civilian vehicles. The design's adaptability to challenging terrain conditions, flexibility, portability, and remote controllability signify compliance with military standards. The remote controllability feature allows intervention in emergencies. Additionally, the design aims to minimize waiting times in military settings through its fast-charging capability. EVs also create an advantage in military applications, but high reliability is required. Another advantage of this design is its ability to operate silently, providing a strategic benefit (Khalil et al., 2009).

In the study by Liu and Makaran, they designed a battery charger powered by solar energy, a renewable energy source. DC/DC converter was used in the design. This study was designed mainly for small vehicles. This study encompasses a hybrid charging station powered by renewable energy sources, particularly solar energy. The hybrid charging station also functions as a fast-charging station, constituting the amalgamation of two systems. The first system involves an IGBT rectifier, while the second incorporates an MPPT-enabled DC-DC converterC-DC topologies are utilized in this system. The AC obtained from the grid is converted to direct current (DC) through the IGBT rectifier. Simultaneously, the DC from the MPPT system is combined with the rectifier output, resulting in the collaborative operation of the two systems. This feature allows for installation in any desired location without the necessity of grid power. The presence of grid energy at the installation site is optional.

METHODS

Renewable Energy

The energy demand, initiated with the Industrial Revolution, has brought about specific challenges due to the use of fossil fuels and the impact of a growing population. The production of most goods and associated logistical activities heavily relies on fossil fuel resources, leading to environmental problems and hazardous carbon emissions affecting the atmosphere. As alternatives to these issues, environmentally friendly and clean energy sources, known as renewable energy sources, have gained increasing significance (Öymen et al., 2020). Geothermal, hydroelectric, solar, biomass, and wave energy are examples of renewable energy sources. These sources are becoming more crucial as countries invest more in their utilization due to their inexhaustible nature (Bekar et al., 2020).

Solar energy, one of the renewable energy sources, is utilized not only for heating, cooling, and obtaining hot water but also for electricity generation. The most common method of electricity production from solar energy involves photovoltaic applications using solar cells. To harness energy from solar radiation effectively, it is ideal to be located between latitudes of 45° north and south (Karamanav et al., 2007). Turkiye, geographically situated between 36-42° north latitudes, enjoys an advantageous position for solar energy compared to many other countries. According to the Turkiye Solar Energy Potential Atlas (GEPA), created to maximize the utilization of solar energy and assess its potential in electricity generation, Turkiye has an annual average of 2741 hours of sunlight and a total energy amount of 1527 kWh/m^2 per year (Arca et al., 2022). Figure 3 provides Turkiye's monthly solar radiation values.

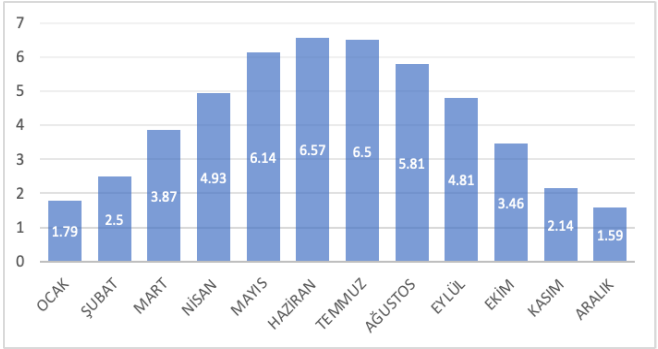

Figure 3. The solar radiation values for Turkiye by month (kWh/m^2) (URL-2, 2022)

Electrical Equivalent Circuit Model of Solar Cells

The similarity of solar cells to diode structures can be referred to as photodiodes due to their resemblance to diode currents, according to Equation 1. For the electrical equivalent circuit of a solar cell, a single-diode electrical circuit model is preferred for its simplicity and reliability (Karabaş et al., 2019). This choice is due to the complexity of the dual-diode structure and the lack of a significant difference in the modeling stage (King et al., 2004). Figure 4 illustrates the single-diode equivalent circuit for a solar cell.

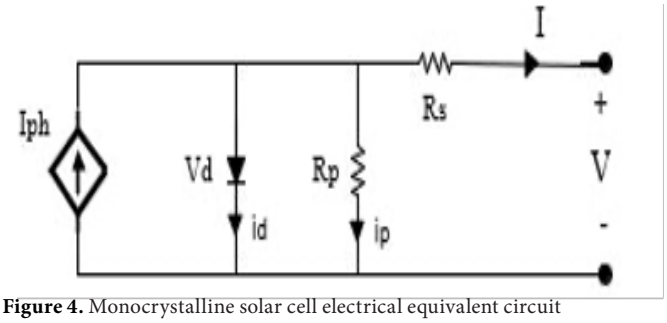

Figure 4. Monocrystalline solar cell electrical equivalent circuit

In the figure's equivalent circuit of the solar cell, Iph represents the solar energy photon current, Vd the diode, Rp the parallel resistance, and Rs the series resistance. Since Rp and Rs introduce conduction losses, they negatively impact the cell efficiency. Rp is the resistance that reflects defects due to the crystal structure of the cell, while Rs represents the internal resistance of the solar cell. The series-connected Rs resistance affects the short-circuit current, while the parallel-connected Rp resistance influences the open-circuit voltage (Ozcalik et al., 2013). I and V indicate the current and voltage of the solar cell. The adapted Iph current equation, according to Figure 4, is provided below when a load is connected to the solar cell contacts. The I current is the generated current of the solar cell. The formulas containing calculations for the solar cell are specified in Equations (1), (2), (3), (4), and (5).

$$I = Iph - id - ip \tag{1}$$

$$id = I_0\left(e^{\frac{qV_D}{mkT}} - 1\right) = I_0\left(e^{\frac{q(V_{pv}+I.Rs)}{mkT}} - 1\right) \tag{2}$$

$$ip = \frac{V_D}{R_p} = \frac{(V_{pv}+I.R_s)}{R_p} \tag{3}$$

$$I = Iph - I_0\left(e^{\frac{q(V_{pv}+I.Rs)}{mkT}} - 1\right) - \frac{(V_{pv}+I.R_s)}{R_p} \tag{4}$$

$$I = Iph.(1 + C_0(T - 300)) - I_0\left(e^{\frac{q(V_{pv}+I.Rs)}{mkT}} - 1\right) - \frac{(V_{pv}+I.R_s)}{R_p} \tag{5}$$

In the given equations, I represents the output current, I0 is the diode saturation current, q denotes the elementary charge of an electron (1.602×10^(-19) C), K is the Boltzmann constant (1.381×10$^{(-23)}$ J/K), and T represents the temperature in Kelvin (Bayrak et al., 2012).

Three-Phase PWM Rectifier

A three-phase DGM rectifier is an electronic circuit utilized for converting alternating current to DC through PWM. Its operational principle involves managing current control and voltage transformation by controlling the conduction and cutoff states of three groups of semiconductor switches, similar in structure to the three groups of diodes in a bridge rectifier. The DGM controller adjusts the conduction time of each switch based on the magnitude and phase angle of the input voltage. The longer the conduction time of the switch, the higher the output voltage, and vice versa. Upon adjustment of the conduction time, the average voltage across the switch reaches the desired value throughout the entire cycle. Adding a capacitor to the output minimizes voltage fluctuations (Zhou, 2023).

IGBT rectifiers are devices that drive the applied alternating current to convert it into the desired DC through PWM technique. In previous applications, rectifiers developed using thyristors had lower efficiency, lower power factors, insufficient switching frequencies, and higher harmonic distortions, making using IGBT rectifiers more advantageous. IGBT rectifiers have been employed in the design of the charging station, aiming for high efficiency and a higher power factor. An IGBT rectifier consists of four elements: a transformer, a semiconductor switch IGBT, a capacitor, and an inductor.

In the circuit depicted in Figure 5, Vin represents the input voltage, Q1, Q2, Q3, Q4, Q5, and Q6 denote the IGBT semiconductor switching elements, L represents the inductance, C represents the capacitor, R represents the load resistance, Io represents the output current, and Vo represents the output voltage. The IGBTs are switched to adjust the desired DC at the system's output.

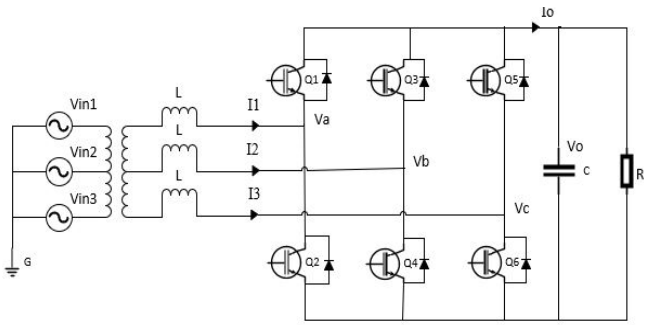

Figure 5. Three-phase PWM rectifier topology

The control method for the three-phase PWM rectifier is provided in Figure 6. The Proportional-Integral (PI) control method adjusts the gain by comparing the externally provided reference DC information with the output DC information, allowing the desired DC to be set at the output. The Control Unit transmits the error value obtained by comparing the rectifier output voltage with the reference input voltage generated using a sine wave table, along with the DC voltage value and the "Modulation Index" value, which will be obtained using the "Duty Cycle" value. Multiple methods are used for switching semiconductors IGBTs in PWM rectifiers. Some of these methods are as follows.

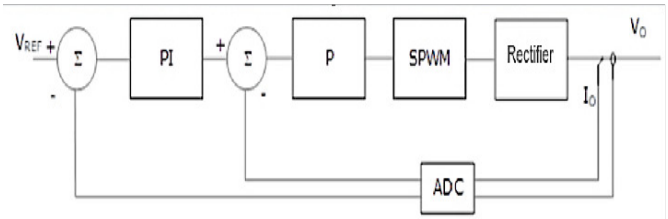

Figure 6. The control method of the PWM rectifier

Hysteresis current control (HCCPWM): The hysteresis current-controlled PWM method is one of the preferred control methods due to its direct control of current, simplicity, and short dynamic response time. This control method calculated the error ratio between the actual current and the reference current generated by the control algorithm. Semiconductor devices remain in conduction within the specified maximum and minimum limits for the calculated error value, allowing the current to flow. When the current error value reaches certain limits, signals that decrease or increase the current value are sent to the switching element. Figure 7 illustrates the current error and PWM signal.

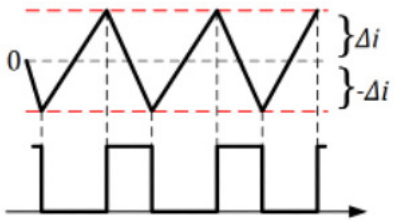

Figure 7. Current error in hysteresis current control

A PI controller is employed as the system control algorithm. The voltage error information from the DC output is controlled through the PI controller, determining the magnitude of the current coming from the grid. The voltage measured from the grid allows the determination of the grid angle through the phase-locked loop (PLL). Additionally, it ensures the creation of a synchronous current reference with the grid. The grid current is subtracted from the reference current for the current error. This error value determines the switching states (Evren et al., 2021).

Space vector pulse width modulation (SVPWM): Another technique used in the semiconductor switching of power electronic devices in industrial applications is the SVPWM technique. This technique offers advantages such as a constant output voltage and a high power factor with fewer harmonics in the output voltage. Unlike other techniques, SVPWM utilizes a reference vector. In operating a three-phase system, the SVPWM for SVPWM, similar to the structure in Figure 5, has eight conduction states for three of the six switching elements for the upper switches. The lower switches operate inversely to the upper switches.

In Figure 8, the vector representation for the eight possible switching states of the rectifier is provided. The reference vector is determined in the region where the calculation result falls and is closest to three neighboring vectors (Yüksek et al., 2019).

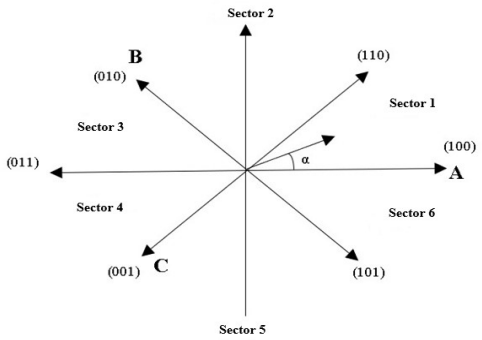

Figure 8. Voltage vector parts of a space vector according to the network

Sinusoidal pulse width modulation (SPWM): The SPWM technique is the industry's most widely used switching technique compared to the other two techniques. This technique is based on a carrier-based modulation technique. In this technique, the angle of the obtained reference current is phase-shifted by the angle between the desired voltages. This waveform is compared with a high-frequency carrier triangular wave to generate the necessary PWM pulses for switching. Instead of keeping the width of all pulses constant in this modulation technique, it is varied proportionally to the amplitude of a sinusoidal wave considered as the center of each pulse. At the same time, distortion factor and low-order harmonics are significantly reduced with this method. According to literature studies, the SPWM signal exhibits better performance than other PWM signals, as it has fully open and closed states of the switching element despite having an equal switching frequency to the carrier wave. The efficiency of the rectifier is improved through the control method based on the comparison made with the SPWM method. Other advantages of this method include decreasing the Total Harmonic Distortion (THD) of the output current and voltage. Figure 9 illustrates the generation of the required PWM signal with a triangular carrier wave.

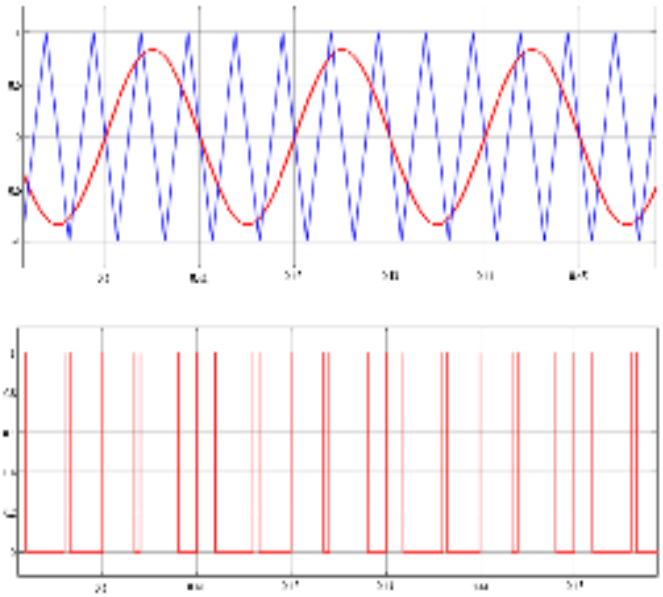

Figure 9. PWM signal compare of one phase for three phase rectifier

In this study, the SPWM method has been employed as the switching control method for the rectifier. Information regarding the simulation and implementation conducted using this method is provided in the Results section. The required PWM signal is generated by comparing the low-frequency sine wave with the high-frequency (10-20 kHz) carrier triangular signal. When the carrier triangular signal is smaller than the sine wave, the output voltage, Vout, equals Vdc. Otherwise, the output voltage is equal to -Vdc. This calculation is shown in Equation 6.

$$I = \begin{cases} +V_{DC}, V_{reference} > V_{carrier} \\ -V_{DC}, V_{reference} < V_{carrier} \end{cases} \quad (6)$$

The pulse widths of the SPWM waveform are calculated as indicated in Figure 10.

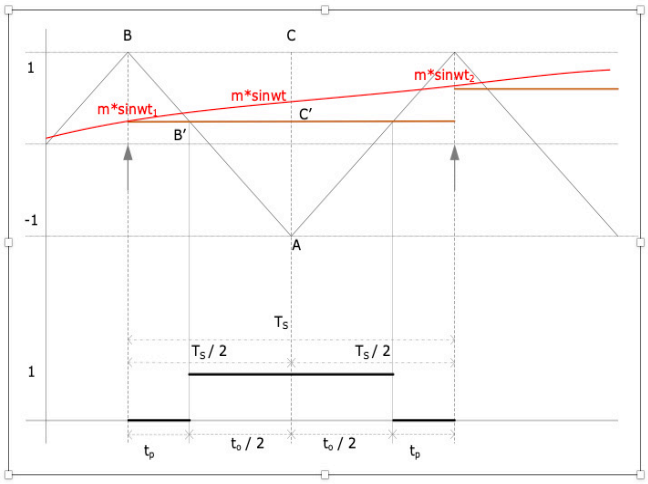

Figure 10. SPWM pulse width calculation method

$$B'C' = (AC' * BC) / AC \quad (7)$$

$$m = VRef / VC \quad (8)$$

$$t0 = Ts/2 * (1 + m * \sin(wt1)) \quad (9)$$

$$w = 2\pi f_{AC} \quad (10)$$

$$tp = Ts/4 * (1 - m * \sin(wt1)) \quad (11)$$

$$Ts = 1/Fs \quad (12)$$

Here, m represents the modulation index, f is the measurement frequency, and Ts denotes the measurement time. Also, sampling has been done for a specific time interval. The calculated values define the time that needs to be applied due to the switching.

Buck-Boost Type DC-DC Converter

Switching DC-DC converters provides a regulated DC output by adjusting the DC input to the desired value using the PWM method. Although this system is quite diverse, it is commonly used in thermal power plants, the iron and steel industry, solar power plants, and many other places. There are three types: step-down, step-up, and both step-down and step-up. Additionally, there is a type with MPPT capability. In the conducted study, two DC-DC converters were used. The first one is a step-down and step-up type DC-DC converter with MPPT capability. The other one is a buck-boost type DC-DC converter without MPPT capability. Generally, these converters consist of a semiconductor device (IGBT, MOSFET, BJT), inductor, diode, and capacitor elements. Figure 11 illustrates the schematic of a step-down and step-up DC-DC converter. In the circuit shown, Vs represents the input voltage, S the semiconductor switching element, D the diode, L the inductor, C the capacitor, R the load resistance, and Vo the output voltage. In a buck-boost circuit, the input voltage can be lower than, higher than, or equal to the output voltage. It is necessary to examine the conduction (S on) and cutoff (S off) states of the S switch in the circuit analysis. In Figure 12, the conduction and cutoff durations are shown, Equation (13) provides the duty cycle calculation, and Equation (14) presents the theoretical output voltage formula for the converter.

$$p = \frac{t_{on}}{t_{on}+t_{off}} = \frac{t_{on}}{Ts} \quad (13)$$

$$V_o = \frac{p}{1-p} * V_s \quad (14)$$

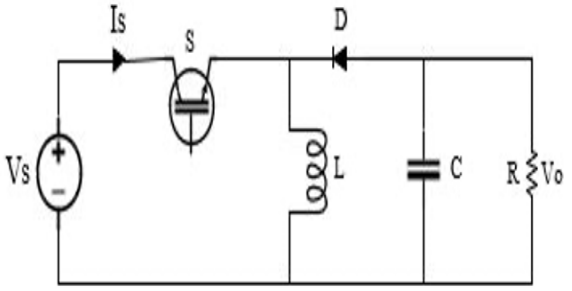

Figure 11. Buck-boost DC-DC converter circuit

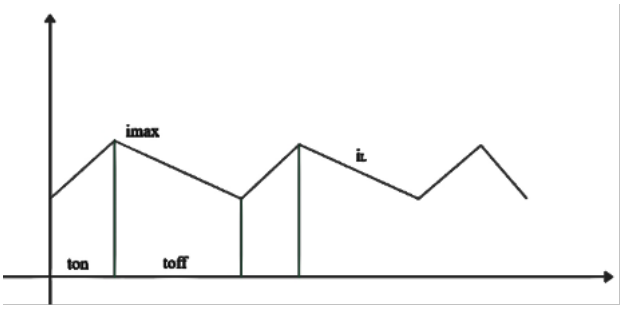

Figure 12. Buck-boost converter duty cycle

Here, p represents the duty cycle, Vo is the output voltage, Vs is the input voltage, t (ton and toff) is the on and off times of the S switch, and Ts is the switching period. The duty cycle, denoted by P, can take values between 0 and 1. Different voltage levels are obtained for different P values. When P < 0.5, it is a step-down type; when P > 0.5, it is a step-up type (Çalışkan et al., 2017). Capacitors and inductors are used to reduce the fluctuations in the converter's output. The inductance value used to minimize the reduction in output current should be adjusted.

The expression describing the inductor current and the voltage across the circuit when the switch is ON is given in Equation (15).

$$\begin{cases} \frac{di_L}{d_t} = \frac{1}{L}(V_s) \\ \frac{dv_0}{d_t} = \frac{1}{C}(-\frac{V_o}{R}) \end{cases} \quad ,0 < t < dT,\ S:ON \quad (15)$$

The expression describing the inductor current and the voltage across the circuit when the switch is OFF is given in Equation (16).

$$\begin{cases} \frac{di_L}{d_t} = \frac{1}{L}(V_o) \\ \frac{dv_0}{d_t} = \frac{1}{C}(-i_L - \frac{V_o}{R}) \end{cases} \quad ,dT < t < T,\ S:OFF \quad (16)$$

To achieve the desired output values for a buck-boost type DC-DC converter, the output voltage, capacitor capacitance, and inductor inductance must be adjusted. The circuit's output voltage is given in Equation (17), the value of the

inductor to be used is given in Equation (18), and the value of the capacitor to be used is given in Equation (19) (Dogra et al., 2014).

$$V_o = DV_S/(1-D) \quad (17)$$

$$L_o = (1-D)V_o/(\Delta I_{LO})f_s \quad (18)$$

$$C_o = D/\{(Rf_s)(\Delta V_{CO}/V_o)\} \quad (19)$$

System Setup and Operating Structure

Electric vehicle hybrid charging station control system: The structure for the hybrid charging station is provided in Figure 13. The hybrid charging station comprises one rectifier, two buck-boost converters, batteries, and photovoltaic panels. Energy for the EV in the hybrid charging station is supplied in two ways: first, through solar energy, and second, from the grid. The energy obtained from the sun and charging the EV also charges the batteries in the storage unit simultaneously. This way, when there is no charging process, the energy obtained from the sun is preserved. In cases where solar energy is not sufficient for the charging process, the charging process is provided through the batteries, and when both are not sufficient, the charging process is ensured with the DC rectified from the grid through the rectifier.

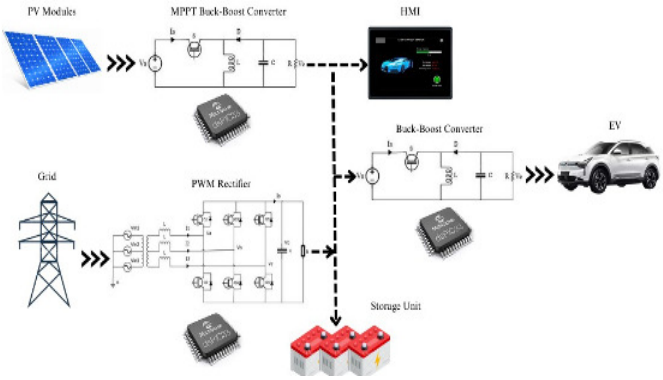

Figure 13. Hybrid charge station topology

These adjustments in the system ensure the maximum use of energy from the sun and are monitored and controlled in real-time through the human machine interface (HMI). A 10.1" TFT All-in-One computer is used as the HMI unit. The PWM rectifier performs the AC-DC conversion, converting 380V AC to 408V DC. The energy obtained from the sun, with the MPPT feature of the buck-boost converter, tracks the maximum power point to produce 408V DC at its output. The second buck-boost converter used in the system provides the DC required for the EV. The system's output can be adjusted from 0 to 400V DC. Control in the PWM rectifier and DC-DC converters is provided by the dsPic33ep256mc206 microcontroller.

PV modules: The system utilizes 60 monocrystalline solar panels with a power rating of 450W each. Selecting monocrystalline solar panels is attributed to their higher efficiency, longer lifespan, lower thermal losses, and aesthetic appeal. Additionally, the panels are connected in series and parallel configurations, with 10 panels in series and 6 in parallel, producing approximately 460V DC at the output. Considering an output of 10A per panel, it is observed that the system can deliver a total current of 600A. Furthermore, each panel has a power output of 450W, as indicated in Table 2. Cumulatively, the system boasts a total power of 27,000 watts, showcasing its substantial energy capacity. The specific characteristics of the panels are provided in Table 2.

Table 2. The electrical characteristics of the used solar panel in the system

Description	Values
PV panel maximum power (W)	450
Maximum power point current (A)	10.6
Open circuit voltage (V)	46.6
Maximum power point voltage (V)	42.3
Module efficiency (%)	20.3

Storage unit: The storage unit is used to ensure the continuity of the system and to meet the energy needs in cases where solar energy is insufficient. The system uses 30 VRLA (Valve Regulated Lead Acid) batteries. The charging process of the batteries is provided by the energy generated by the PV modules. The Buck-Boost converter uses the energy stored in the batteries to charge the EV in case of need. The technical specifications of the VRLA batteries are given in Table 3.

Table 3. The technical specifications of the VRLA battery used in the system

Description	Values
Nominal voltage	12V
Capacity	100A
Charge current	20A
Nominal charge voltage	13.6V
Boost charge voltage	14.2V

HMI: A typical display unit, the HMI, monitors system measurements and adjusts them within the desired range. The HMI consists of a TFT panel, a processor, and a remote communication module. Through the HMI, the control process is carried out, and the system has the task of turning off the rectifier section based on the solar energy potential and operating the DC-DC converters. The control unit in the system is the HMI. The image belonging to the HMI is presented in Figure 14.

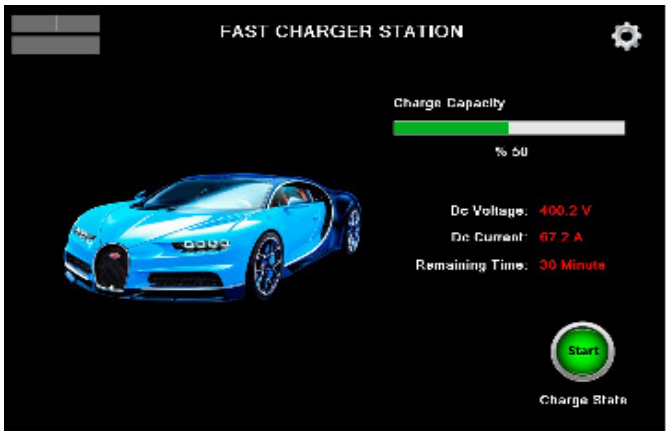

Figure 14. HMI screen of hybrid charge station

Buck-boost type DC-DC converter design: The step-up/step-down type DC-DC converter in the circuit in Figure 15 is used for two purposes. The first converter transforms the 250V to 460V DC from the PV panels into 408V DC required for charging the batteries at the output. This DC-DC converter, unlike the others, has the MPPT feature. This feature is implemented only in software without the need for any hardware changes. With MPPT, the maximum power

point of the energy obtained from the sun is determined. The second converter has an input voltage range of 300V to 408V DC, which will not discharge the batteries deeply. It uses the voltage from the batteries and generates 400V DC at the output to charge the EV batteries. The system uses IGBT, coil, diode, and capacitor as switching elements.

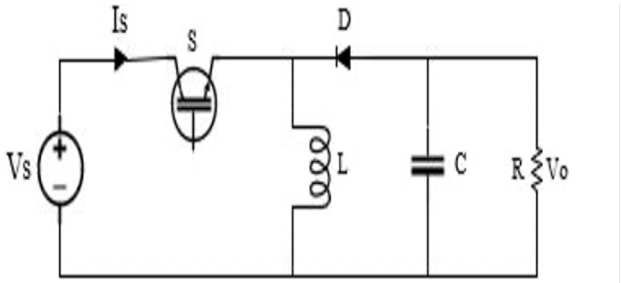

Figure 15. Buck-boost DC-DC converter circuit

If we consider that the PV output voltage is 400V DC, the required duty cycle can be calculated using Equation (14) as follows:

$$V_o = \frac{d}{1-d} * V_{in} \Rightarrow \frac{V_i}{V_o} = \frac{400V}{408V} = 0.98 \Rightarrow d = 0.505 \text{ duty cycle}$$

The duty cycle of the IGBT switch is calculated as 50.5%. The minimum current of the circuit is determined to be 10A. The switching frequency is chosen as 20 kHz. The required inductance value can be calculated using Equation (18) as follows:

$$L_o = (1-D)V_o/(\Delta I_{LO})f_s \Rightarrow (1-0.505) * 408/10 * 20 * 10^3 = 1.01\,mH$$

Here, the calculated value is approximately 1 mH. Assuming a load value of 100 ohms for the system's start and considering a ripple of 100mV in the output voltage, the required capacitor value can be calculated using Equation (19) as follows:

$$C_o = D/\{(Rf_s)(\Delta V_{CO}/V_o)\} = 0.505/\{(100 * 20 * 10^3)(100 * 10^{-3}/408)\} = 1030\ uF$$

PWM rectifier design: In the circuit shown in Figure 16, the PWM rectifier converts 380V three-phase alternating current from the grid into 408V DC. IGBT is used as the switching element in the circuit. In addition to this, a transformer, inductors, capacitors, and diodes are used as isolation and voltage reduction components. In this case, the storage unit's batteries represent the load resistance.

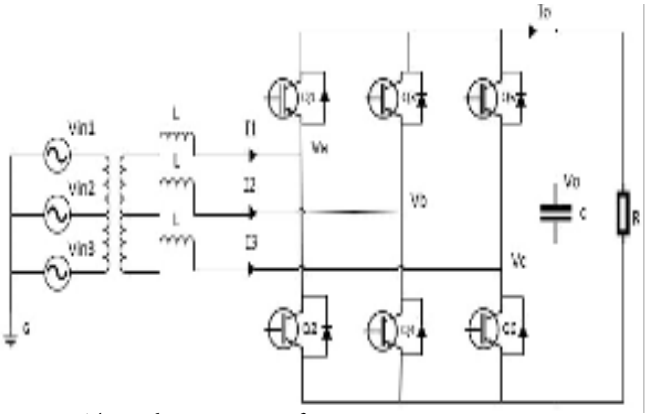

Figure 16. Three-phase PWM rectifier circuit

The role of the rectifier during the system's operation is to become active when the energy obtained from the sun and stored in the batteries is insufficient, thus performing the charging process.

The PWM rectifier has a power factor (PF) exceeding 95%. The current harmonic is below 5%. The switching frequency of the PWM rectifier is 16 kHz. The calculated period for this frequency value is determined using Equation (12) as follows:

Fs = 16 kHz

$$Ts = 1/Fs = 1/(16 * 10^3) = 62.5\ us$$

RESULTS

PWM Rectifier Simulation Study

Simulations were conducted based on the theoretical values of the PWM rectifier used in the system. In this study, inductors, capacitors, transformers, and switching elements were assumed to be ideal. As depicted in Figure 17, the circuit simulation was implemented using Matlab/Simulink.

The simulation results are presented in Figure 16. The AC signal from the input has been converted to 408V DC through the PWM rectifier. The IGBT switching frequency is selected as 16 kHz. The corresponding triangular wave signal generates the main PWM pulses. The modulation index is 30.5%. The simulation graphs for input voltage and current are shown in Figure 17, indicating that the fluctuation in the output voltage of the PWM rectifier is close to 100 mV. Additionally, the rectifier is loaded with a 5-ohm resistor. The graphs for output voltage and current are provided in Figure 18. The IGBT switching signals generated by the SPWM are shown in Figure 19.

As shown in Figure 18, the output voltage is specified as 400V DC. The load at the output draws approximately 82A current. Both current and voltage have fluctuations of up to 100mV and 100mA. The system starts with a soft start, reaching nominal values in 0.3 seconds. Additionally, Figure 20 provides the switching PWM pulses. Feedback information is obtained from the input voltages and compared with a triangular wave at a frequency of 16 kHz to enable the IGBTs to switch according to the SPWM method. This result is multiplied by the modulation index, allowing controlled adjustment of the SPWM for the desired output voltage.

Buck-Boost Type DC-DC Converter Simulation Study

A simulation study has been conducted based on the theoretical values of the DC-DC converter used in the system. This study considered the inductor, capacitor, and switching elements ideal. The circuit simulation, as shown in Figure 21, was implemented using the Matlab/Simulink.

For the initial condition, the resistance value is calculated below to allow a minimum current, also known as the damper load, to pass through the resistor. The resistance value is calculated for a 408V charging voltage and a 4A load resistance.

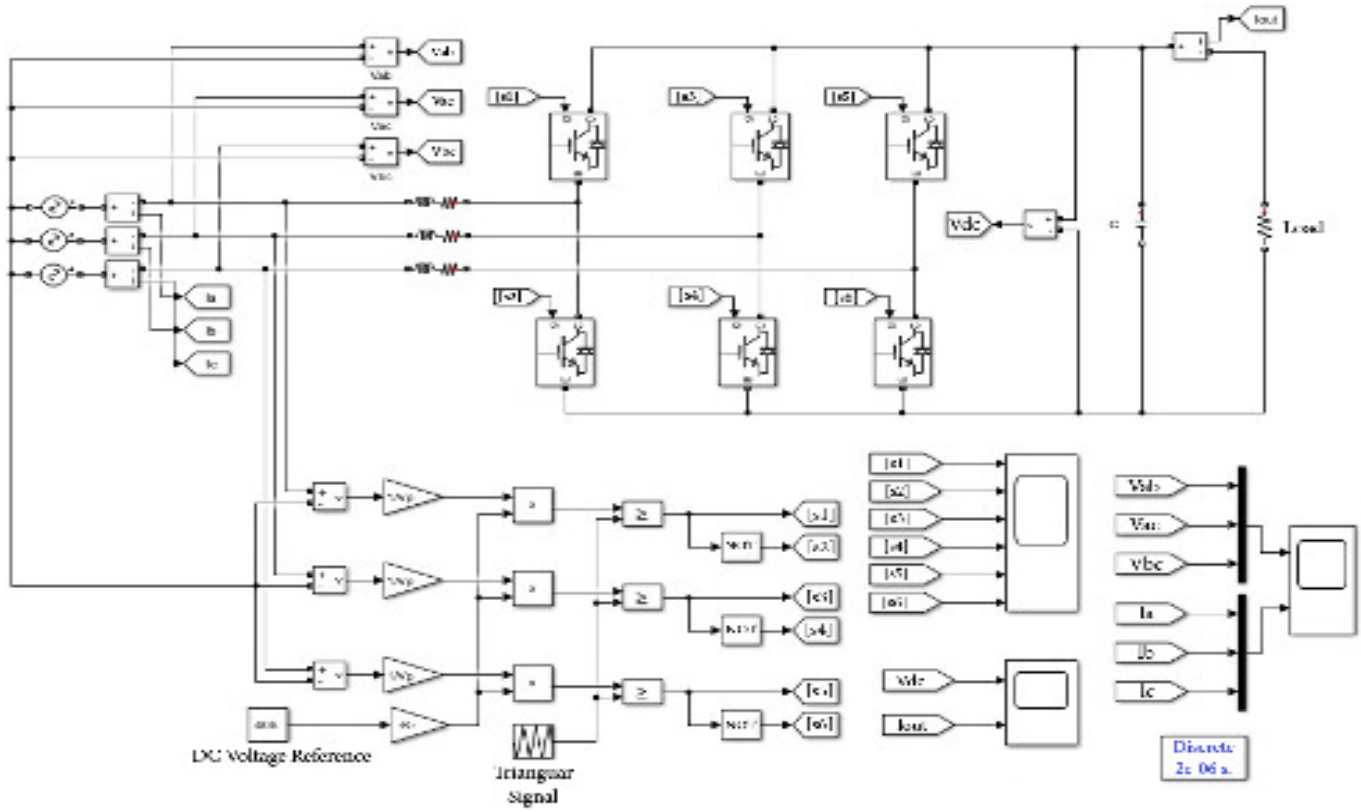

Figure 17. Three-phase PWM rectifier circuit (Detailed)

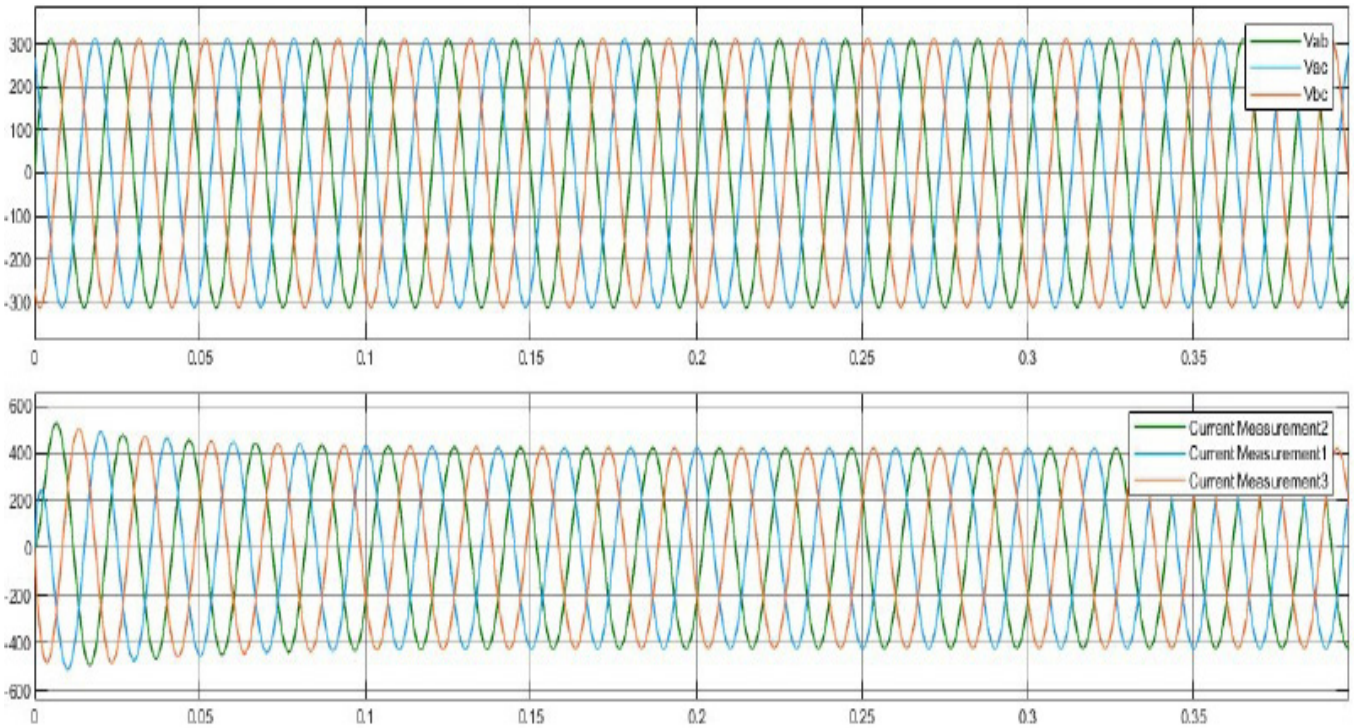

Figure 18. PWM rectifier input voltage and currents

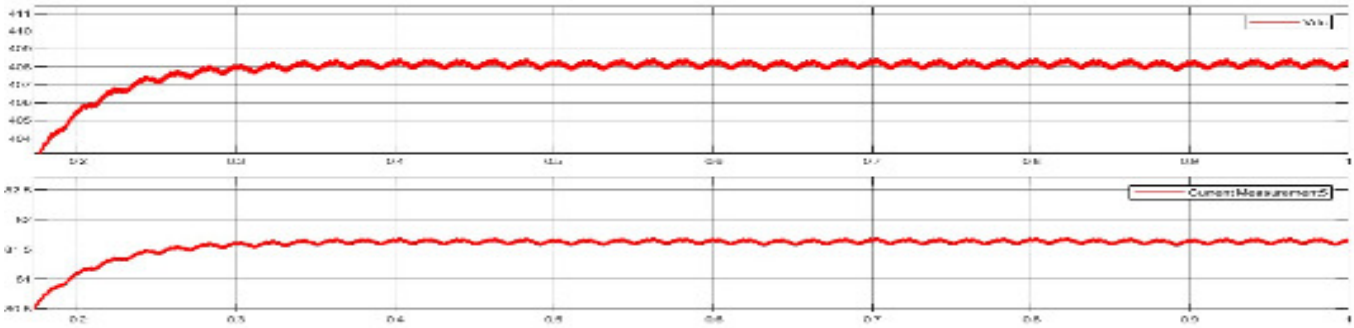

Figure 19. PWM rectifier output voltage and currents

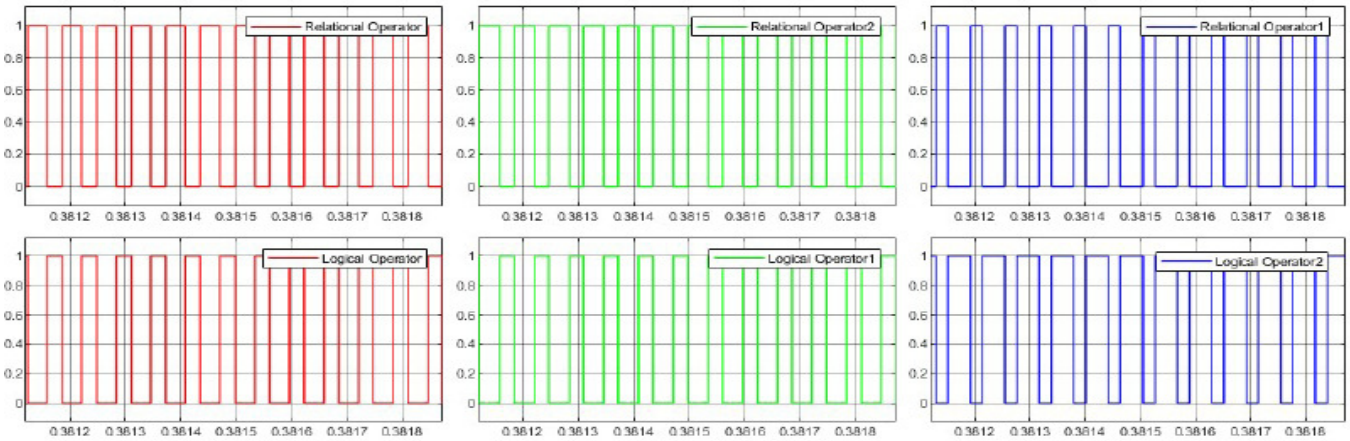

Figure 20. PWM rectifier for 6 IGBT SPWM pulses that produced with modulation index

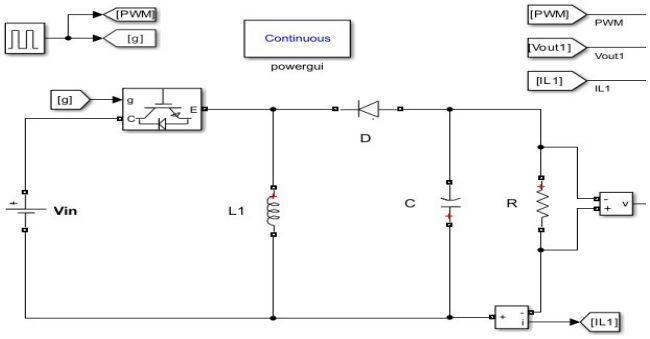

Figure 21. Buck-boost type DC-DC converter simulation model

$$\text{Ryük} = \text{Vnominal} / \text{Imin} = 408 / 4 = 102\ \Omega$$

In the simulation conducted for the buck-boost converter, a 408 Ω resistor was used as the load, and the calculated capacitor and inductor values were utilized. The input voltage was set to the nominal voltage of 400V DC from the panels. The IGBT switching frequency was chosen as 20 kHz, and the duty cycle period was set to the calculated value of 50.5%. The simulation results are presented in Figure 22.

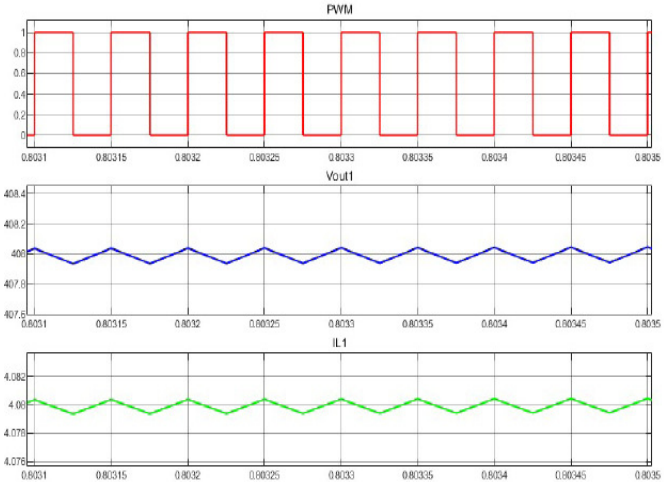

Figure 22. DC-DC converter simulation graphics

As a result of the simulation, the PWM signal, output voltage, and output current related to the duty cycle of the IGBT switch were obtained, as shown in Figure 18. The IGBT was driven with a 50.5% duty cycle. The load voltage has a ripple voltage of 100 mV, while the load current is at a value of 4A with a 100 mA fluctuation.

Hybrid Charging Station Experiment and Implementation

The experimental and implementation phase of the hybrid charging station was conducted using Matlab/Simulink simulation. The study involved images of the 380V AC power source, PWM rectifier, DC-DC converter, Transformer, Power Supply, Mainboard, IGBTs, and HMI unit, as depicted in Figure 19.

As seen in Figure 23, the circuit consists of several electrical components. Additionally, a 100A MCCB (Moulded Case Circuit Breaker) has been utilized to protect any short circuits in the system's inputs and outputs. For the storage unit, 30 units of 12V VRLA batteries have been employed to charge the EV. Fluke brand measurement tools were used to measure input and output voltages. The switching frequencies were monitored with an oscilloscope.

Before connecting the application circuit to regular EVs, tests were conducted under load in a test environment. These tests were conducted based on the voltage and current values simulated. Isolated driver circuits were used to drive the IGBTs. All power supplies were provided from the supply card shown in Figure 19. The power supplies in the system are divided into 12V and 5V. In Figure 24, a 408.0V DC is observed at the outputs of both the PWM rectifier and the DC-DC converter.

In Figure 25, the switching frequency of the DC-DC converter is provided. The duty cycle period starts as a soft start at 50.5%.

The simulation and application results show that a 408V DC output is provided for the PWM rectifier with a fluctuation level below 1%. It is also shown in Figure 20. Additionally, the switching pulses for the PWM rectifier are shown in Figure 26. The IGBTs are driven with a soft start, ensuring work safety by shutting down the system in case of any danger. When the system's efficiency is theoretically calculated, it exceeds 95%, aligning well with the practical application. The Buck-Boost type DC-DC converter converts the voltage obtained from solar energy to 408V DC to charge the batteries in the storage unit and serves as an energy source for the second converter.

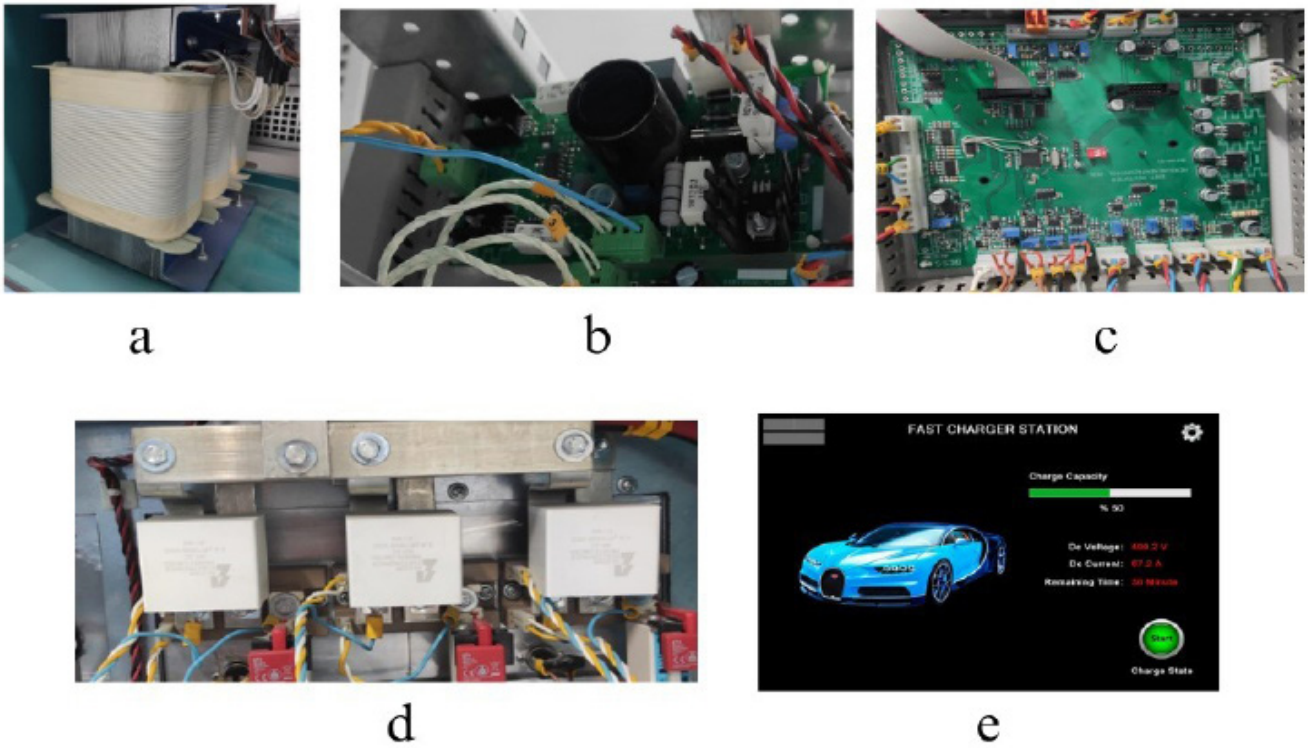

Figure 23. (a) Transformer, (b) power supply card, (c) main board, (d) IGBTs, (e) HMI unit

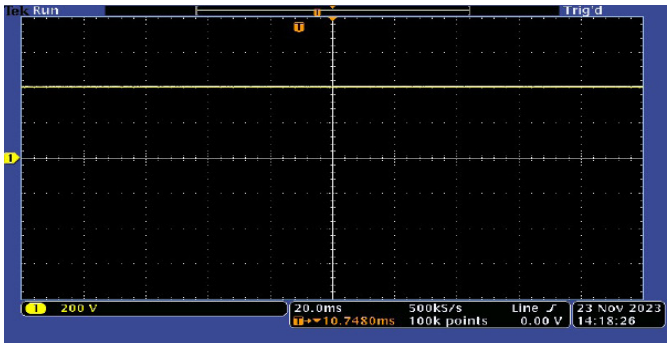

Figure 24. PWM rectifier output voltage with oscilloscope

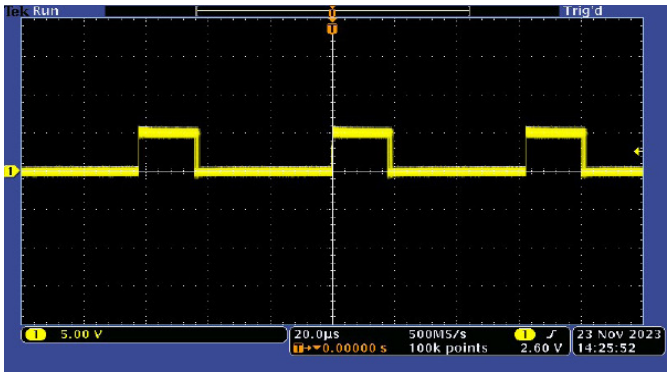

Figure 25. DC-DC converter PWM pulses

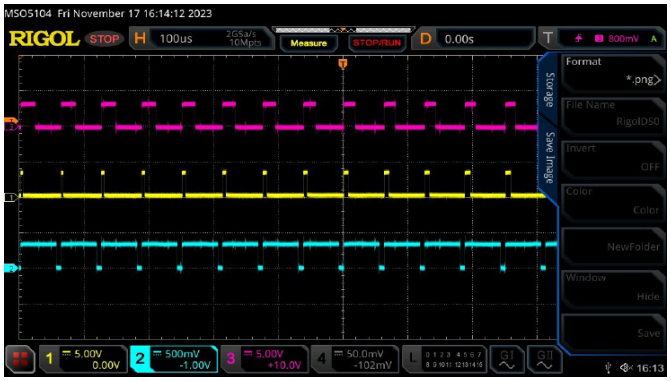

Figure 26. PWM rectifier IGBT SPWM pulses for three-phase

DISCUSSION

The dependence on vehicles using fossil fuels for transportation, which is significant in our lives, harms the environment and human health. Vehicles utilizing fossil fuels also contribute significantly to carbon emissions, posing a substantial threat to the atmosphere and impacting global climates. For these reasons, the number of environmentally friendly EVs is increasing daily. However, this rise raises questions about the charging infrastructure and the suitability of the electrical grid.

This study transfers the DC generated through PV modules to the storage unit using a buck-boost type DC-DC converter. The batteries in the storage unit charge, and fully charged batteries are sufficient to charge multiple vehicles. The hybrid charging station employs a fast-charging method, offering up to 70% charge in half an hour if the vehicle's specifications allow. In cases where solar energy is insufficient, and the storage unit is not enough for vehicle charging, the grid-powered rectifier is activated. The system contributes to energy savings by utilizing solar power.

Hybrid charging stations have no space limitations and can be used by individuals or companies. They are suitable for military vehicles in remote areas, providing independence from the grid. The system operates based on renewable energy without dependence on the grid. Future research can focus on increasing battery capacities and providing charging capabilities for EVs supporting up to 1000 VDC. Advancements in fast-charging technologies can increase current flow and allow for higher power levels. Increasing the number of PV modules can power multiple vehicles with solar panels alone. Bidirectional rectifiers can transfer excess energy back to the grid, incorporating different control structures and artificial intelligence for optimization.

CONCLUSION

The development and implementation of hybrid charging stations represent a promising solution to address the environmental and health concerns associated with traditional fossil fuel-powered transportation. By harnessing solar energy through photovoltaic modules and employing an innovative buck-boost DC-DC converter, this study demonstrates a sustainable approach to charging EVs while minimizing reliance on the conventional grid. The hybrid charging stations not only contribute significantly to reducing carbon emissions but also offer flexibility for use in diverse settings, including remote areas and military applications. The incorporation of fast-charging technology, coupled with the ability to draw power from both solar and grid sources, ensures a reliable and efficient charging infrastructure. As we look toward the future, further research and advancements in battery capacities, fast-charging technologies, and bidirectional rectifiers, combined with artificial intelligence optimization, hold the key to enhancing the viability and scalability of this eco-friendly solution.

ETHICAL DECLARATIONS

Referee Evaluation Process

Externally peer-reviewed.

Conflict of Interest Statement

The authors have no conflicts of interest to declare.

Financial Disclosure

The authors declared that this study has received no financial support.

Author Contributions

All of the authors declare that they have all participated in the design, execution, and analysis of the paper, and that they have approved the final version.

Acknowledgments

I would like to express my gratitude to my thesis advisor, Assoc. Prof. Dr. Atilla Ergüzen, who provided unwavering support and guidance with his knowledge and experience in the preparation of my article.

I extend my thanks to my father Talip Kuzu and my mother Nadime Kuzu, who have been with me at every stage of my life and never withheld their support. I am also grateful to my wife Burcu Kuzu and my daughter Asya Meva Kuzu, who supported and assisted me throughout my master's education. Special thanks to my sister Sena Kuzu, who has always been by my side and never hesitated to offer her support and encouragement.

REFERENCES

1. Angelov, G., Andreev, M., & Hinov, N. (2018, May). Modeling of electric vehicle charging station for DC fast charging. In 2018, the 41st International Spring Seminar on Electronics Technology (ISSE) (pp. 1-5). IEEE.
2. Arca, D., & Keskin Çıtıroğlu, H. (2022). Güneş enerjisi santral (GES) yapım yerlerinin CBS dayalı çok kriterli karar analizi ile belirlenmesi: Karabük örneği. *Geomatik*, 7(1), 17-25.
3. Bayrak, G., & Cebeci, M. (2012). 3.6 kW gücündeki fotovoltaik generatörün matlab simulink ile modellenmesi. *Erciyes Üniversitesi Fen Bilimleri Enstitüsü Fen Bilimleri Dergisi*, 28(3), 198-204.
4. Bekar, N. (2020). Yenilenebilir enerji kaynakları açısından Türkiye'nin enerji jeopolitiği. *Türkiye Siyaset Bil Derg*, 3(1), 37-54.
5. Çalışkan, A., Ünal, S., & Orhan, A. (2017). Buck-boost dönüştürücü tasarımı, modellenmesi ve kontrolü. *Fırat Üniv Mühend Bil Derg*, 29(2), 265-268.
6. Çetintaş, H., Bicil, İ. M., & Türköz, K. (2017). Türkiye'de enerji üretiminde fosil yakıt kullanımı ve CO2 emisyonu ilişkisi: bir senaryo analizi (No. 2017-002, pp. 1-12). EconWorld Working Paper Series.
7. Dericioglu, C., Yirik, E., Unal, E., Cuma, M. U., Onur, B., & Tumay, M. (2018). A review of charging technologies for commercial electric vehicles. *Int J Advanc Automotive Technol*, 2(1), 61-70.
8. Dogra, A., & Pal, K. (2014). Design of buck-boost converter for constant voltage applications and its transient response due to parametric variation of pi controller. *Int J Innovat Res Sci Engineering Technol*, 3(6), 13579-13588.
9. Eckel, H. G., Bakran, M. M., Krafft, E. U., & Nagel, A. (2005). A new family of modular IGBT converters for traction applications. In *2005 European Conference on Power Electronics and Applications* (pp. 10-pp). IEEE.
10. Gelman, V. (2014). Why there are no IGBT traction rectifiers? In *Proc. of Joint Rail Conference, Colorado Springs, CO, United States*.
11. Gürbüz, İ. B., Özkan, G., & Korkmaz, Ş. (2023). Kırsal kesimde yaşayanların yenilebilir enerji kaynakları ve çevre bilinci üzerine bir araştırma. *Türk Tarım Doğa Bil Derg*, 10(1), 187-195. doi: 10.30910/turkjans.957062
12. IEC. (2010). 61851-1: Electric vehicle conductive charging system-part 1: General requirements. IEC (International Electrotechnical Commission), Geneva, Switzerland.
13. İşen, E. (2021). Comparative study of single-phase PWM rectifier control techniques. *Mugla J Sci Technol*, 7(1), 44-51.
14. Karamanav, M. (2007). Güneş enerjisi ve güneş pilleri (Dissertation). Sakarya University, Turkey.
15. Karabaş, A., & Mengi, O. Ö. (2019). Fotovoltaik güneş panelleri için farklı MGNİ teknikleri kullanılarak bir şarj regülatörünün performansının incelenmesi ve karşılaştırılması. karadeniz fen bil derg, 9(1), 152-175.
16. Khalil, G. (2009). Challenges of hybrid electric vehicles for military applications. In *2009 IEEE Vehicle Power and Propulsion Conference*, (pp. 1-3).
17. King, D. L., Kratochvil, J. A., & Boyson, W. E. (2004). Photovoltaic array performance model (Vol. 8). United States. Department of Energy.
18. Liu, Z., Xie, Y., Feng, D., Zhou, Y., Shi, S., & Fang, C. (2019). Load forecasting model and day-ahead operation strategy for city-located EV quick charge stations.
19. Mouli, G. R. C., Bauer, P., & Zeman, M. (2016). System design for a solar-powered electric vehicle charging station for workplaces. *Appl. Energy*, 168, 434-443.
20. Mouli, G., Venugopal, P., & Bauer, P. (2017). Future of electric vehicle charging. 2017 *International Symposium on Power Electronics (Ee)*. pp. 1-7. Available: 10.1109/pee.2017.8171657 [Accessed 10 December 2019].
21. Ozcalik, H. R., Yilmaz, S., & Kilic, E. (2013). Güneş pilinin bir diyotlu eşdeğer devre yardımıyla matematiksel modelinin çıkartılması ve parametrelerinin incelenmesi. *Kahramanmaraş Sütçü İmam Üniv Mühendislik Bil Derg*, 16(1), 23-29.
22. Öymen, G. (2020). Yenilenebilir enerjinin sürdürülebilirlik üzerindeki rolü. *İst Tic Üniv Sos Bil Derg*, 19(39), 1069-1087.
23. Saber, C. (2017). Analysis and optimization of the conducted emissions of an on-board charger for electric vehicles. Doctoral dissertation, Université Paris Saclay.
24. Sutopo, W., Nizam, M., Rahmawatie, B., & Fahma, F. (2018). A review of electric vehicles charging standard development: study case in Indonesia. In *2018 5th International Conference on Electric Vehicular Technology (ICEVT)* (pp. 152-157). IEEE.
25. Tie, S. F., & Tan, C. W. (2013). A review of energy sources and energy management system in electric vehicles. *Renewable Sustainable Energy Rev*, 20, 82-102.
26. URL-1. (2021). Sources of Greenhouse Gas Emissions. https://www.epa.gov/ghgemissions/sources-greenhouse-gas-emissions (Date of access: 17.11.2023).
27. URL-2. (2022). Energy and Natural Resources Ministry, Sun. https://enerji.gov.tr/eigm-yenilenebilir-enerji-kaynaklar-gunes (Date of access: 26.12.2023).
28. Yüksek, H. İ. (2019). Uzay vektör darbe genişlik modülasyonu yöntemi ile üç faz üç seviyeli doğrultucunun matlab/simulink ortamında modellenmesi (Dissertation). Sakarya Universitesi, Turkey.
29. Zhou, Z., Song, J., Yu, Y., Xu, Q., & Zhou, X. (2023). Research on high-quality control technology for three-phase PWM rectifier. *Electronics*, 12(11), 2417.